



CO₂ switchable deep eutectic solvents for reversible emulsion phase separation†

Feijie Liu,^{ab} Zhimin Xue,^{ib}*^a Xue Lan,^b Zhenghui Liu^{ib}^c and Tiancheng Mu^{ib}*^b

Cite this: *Chem. Commun.*, 2021, 57, 627

Received 20th October 2020,
Accepted 11th December 2020

DOI: 10.1039/d0cc06963a

rsc.li/chemcomm

The concept of CO₂ switchable deep eutectic solvents (DESSs) was proposed and a series of CO₂ switchable imidazole-based deep eutectic solvents (DESSs) was designed. The CO₂ switch mechanism was investigated and the system was used for easy emulsion separation of olive oil from DESSs. The benign CO₂ switchable DESS have great potential applications in dissolution and easy separation.

With the development of green chemistry, green solvents have gained tremendous attention as alternatives of volatile organic solvents.^{1–3} Among various green solvents (*i.e.*, supercritical fluids, ionic liquids, and deep eutectic solvents), deep eutectic solvents (DESSs) are an emerging type.^{4,5} In general, DESSs have similar physicochemical properties to ionic liquids (ILs), but DESSs can be easily synthesized by simply heating a mixture of the different components. The simple synthetic process makes DESSs more advantageous over ILs by avoiding the use of organic solvents and the generation of by-products. Thus, DESSs have been considered as attractive alternatives to ILs in diverse applications,^{6–11} such as separations, catalysis, fabrication of functional materials, and electrochemistry, *etc.* More importantly, the properties of DESSs can be easily tuned by modifying the types and/or the ratio of the components. Thus, DESSs have been recognized as “designer solvents”,¹² which can significantly expand the application of DESSs.

Emulsions are often involved in many chemical, biological, environmental, and engineering processes.^{13–16} For the applications of DESSs, formation of emulsions is also a general phenomenon, especially when they are applied in materials synthesis, chemical

reactions, and extractions. Therefore, phase separation of the DES-based emulsions is of significant importance for the utilization of DESSs from both scientific and practical points of view. Conventionally, phase separation of emulsions can be realized by addition of additives, such as salts, acids, organic solvents, and co-surfactants, *etc.*^{17–20} However, the use of these additives for phase separation of DES-based emulsions would irreversibly change the properties of the DESSs and/or make the separation processes more complex. Consequently, it is highly desirable to develop simple, green and “smart” strategies for the phase separation of DES-based emulsions.

CO₂ is nontoxic, abundantly-available, and easily removable. As a preferred trigger, CO₂ has been applied to switch the physicochemical properties (*e.g.*, hydrophility, viscosity, polarity, and ionic strength) of some solvents,^{21–25} including organic solvents and ionic liquids. Similar to ionic liquids, some physicochemical properties of DESSs could also be modified by the adsorption of CO₂.^{12,26,27} Therefore, it would be an attractive and highly-potential strategy to efficiently and simply realize the phase separation of various substances from DESSs by using CO₂ as the trigger to tune the properties of the DESSs. CO₂-triggered phase separation of DES-based emulsions has not been reported so far.

Based on the reported knowledge, most of the developed CO₂ switchable solvents employed a nitrogenous base.^{21,23–25} Therefore, to form a CO₂ switchable DES-based system, a suitable nitrogenous base would be essential. Imidazole, as a typical nitrogenous base of low cost, has been employed as a hydrogen bonding acceptor (HBA) to form DESSs for SO₂ adsorption,²⁸ and the process was reversible, which is an important merit to generate reversible CO₂ switchable solvent systems. Inspired by the achievements in CO₂-switched solvents and the properties of imidazole, in this work, we desired a family of imidazole-based DESSs by employing imidazole as the HBA and several polyols (*i.e.*, ethylene glycol (EG), glycerol (Gly), 1,4-butanediol (BDO), polyethylene glycol 200 (PEG-200)) as the hydrogen bonding donator (HBD). It was found that phase separation could be easily achieved for the emulsions formed between these imidazole-based DESSs and olive oil by bubbling

^a College of Materials Science and Technology, Beijing Forestry University, No. 35 Tsinghua East Road, Haidian, Beijing 100083, China.
E-mail: zmxue@bjfu.edu.cn

^b Department of Chemistry, Renmin University of China, No. 59 Zhongguancun Street, Haidian, Beijing 100872, China.
E-mail: tcmu@ruc.edu.cn

^c School of Pharmaceutical and Materials Engineering, Taizhou University, 1139 Shifu Road, Jiaojiang, Taizhou 318000 Zhejiang, China

† Electronic supplementary information (ESI) available. See DOI: 10.1039/d0cc06963a

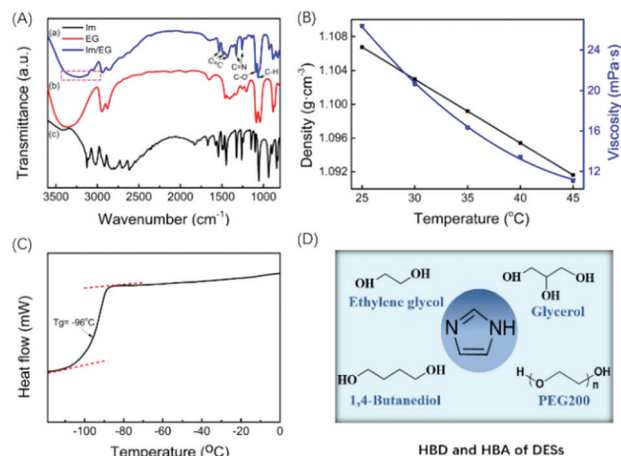


Fig. 1 FT-IR spectra of the imidazole/EG DES (A), viscosity and density of the imidazole/EG DES (B), differential scanning calorimetry (DSC) of the imidazole/EG DES (C), and the chemical structures of the designed imidazole-based DESs (D).

CO₂ at atmospheric pressure. The emulsions would be re-formed after the removal of CO₂ by bubbling N₂. The environment friendly (DES as green solvent and olive oil as naturally occurring product) properties endow this designed system with great potential applications in material synthesis, organic reactions and pollution treatment.

The imidazole-based DESs were prepared by heating a mixture of imidazole and four HBDs (Fig. 1D) with different molar ratios at 30 °C. The prepared DESs with a light-yellow colour (Fig. S1, ESI[†]) were stable at room temperature. To exclude the influence of moisture on the properties of the DESs, they were dried at 50 °C under vacuum with a time of 48 h to ensure low moisture content (<0.3 wt%, Table S1, ESI[†]). The interactions between imidazole and the HBDs were characterized by FT-IR spectroscopy (Fig. 1A). As shown in Fig. 1A, the =C–H bending vibration characteristic peak that appeared at 1057 cm^{−1} for pure imidazole undergoes a blue-shift (1064 cm^{−1}) in the DES formed between imidazole and ethylene glycol (imidazole/EG).²¹ Meanwhile, the C=N stretching characteristic peaks were 1324 and 1261 cm^{−1} for imidazole, while these peaks showed a shift to 1331 and 1254 cm^{−1} in the imidazole/EG DES, respectively.²² Moreover, the peaks at 1668, 1575 and 1541 cm^{−1} assigned to the stretching of C=C, shift to 1535, 1485 and 1428 cm^{−1} in the imidazole/EG DES.^{29,30} In addition, the C–O stretching characteristic peak at 1091 cm^{−1} in pure EG shifted to 1083 cm^{−1} in the imidazole/EG DES.¹⁰ More importantly, the O–H stretching absorption band at 3500–3300 cm^{−1} for pure EG shifted to the red area (3000–3300 cm^{−1}) in the imidazole/EG DES,^{10,31} and meanwhile the band became wider. The above results implied that there were strong intermolecular interactions between the hydroxyl of EG and the imidazole. Similarly, the interactions of the other three DESs were also investigated by FT-IR spectroscopy (see the ESI[†], Fig. S2). These FT-IR results verified the intermolecular interaction between imidazole and the examined HBDs, which were favourable for the formation of DESs.

In general, the fundamental physicochemical properties, especially transport properties (viscosity and density) are very

important parameters for practical applications. Thereby, the viscosities and densities of the DES systems were investigated (Fig. 1B and Fig. S3–S5, ESI[†]). It was found that the viscosities of the synthesized imidazole-based DESs were usually lower than those of most commonly used ionic liquids,³² while all the obtained DESs exhibited slightly higher densities than those of pure water at given temperatures. In particular, the viscosities and densities of the prepared imidazole-based DESs decreased with the increase of temperature (Fig. 1B). In another aspect, the melting points of the obtained DESs were much lower than those of the individual components investigated by differential scanning calorimetry (Fig. S6 and Table S2, ESI[†]), further indicating the formation of the desired DESs. For example, the *T*_g of the imidazole/EG was around −96 °C (Fig. 1C), while the melting points of imidazole and EG were around 90 and −13 °C, respectively.

Emulsions can be obtained when these developed DESs are mixed with olive oil at ambient temperature and pressure, and interestingly, whether the emulsions were formed or not could be controlled by CO₂. Employing the imidazole/EG as an example, the volume ratio of DES/olive oil was fixed at 4:1. In the absence of CO₂, the emulsion system was homogeneous (a in Fig. 2A). When CO₂ was bubbled through the emulsion system at room temperature, it became muddy in less than one minute, which could be considered as the phase transition point, and the absorbed CO₂ amount was 5.4 mmol mol^{−1} DES. The emulsion would be separated into two transparent phases (b in Fig. 2A) after bubbling CO₂ into the system for about 30 min, and the absorbed CO₂ amount was 39.4 mmol mol^{−1} DES for nearly complete phase separation. It was obvious that the upper organic phase was yellow, while the lower phase was light-yellow, indicating the nearly complete phase separation of imidazole/EG-olive oil emulsion. Moreover, no obvious difference was found in the ¹H NMR spectra of the upper phase and the olive oil (Fig. S7, ESI[†]), or the lower phase and the DES

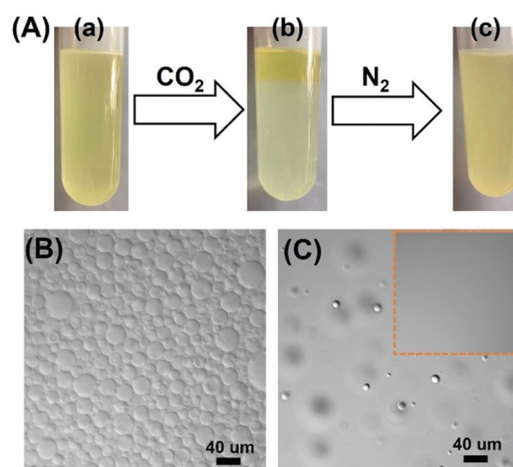


Fig. 2 (A) The photos of the initial imidazole/EG-olive oil emulsion (a), phase separation after CO₂ bubbling (b) and further N₂ injection (c), and the LSCM image of the initial emulsion (B) and the lower phase after CO₂ bubbling with a time of 30 min (C). The insertion in (C) was the lower phase after bubbling CO₂ for 30 min and then standing still for 2 h.

(Fig. S8, ESI[†]), and meanwhile, there were no impurity peaks in the spectra of each phase. These results indicated that the separated phases were pure, which further implied the complete phase separation. More importantly, when CO₂ was removed by the bubbling of N₂ at room temperature for two hours, the emulsion system would be re-formed (c in Fig. 2A). The phenomenon indicated that the property of these prepared imidazole-based DESs could be tuned by CO₂. The microstructures of the initial emulsion and the lower phase (DES phase) after the bubbling of CO₂ were determined by laser scanning confocal microscopy (LSCM), which was a general technique to study the microstructures of the emulsions.³³ It was clear that numerous droplets appeared in the initial imidazole/EG-olive oil emulsion (Fig. 3B), implying that the generated system was not a solution, while no droplets were found in the lower phase after the bubbling of CO₂ (Fig. 3C) because of the occurrence of complete phase separation. The above results indicated that we have successfully synthesized a CO₂-responsive DES-based emulsion, which would have potential applications in various fields, including materials synthesis, chemical reactions, and waste recovery. In addition, the CO₂-responsive phenomenon was also observed in the emulsion system generated between imidazole/EG DES and peanut oil, while unstable emulsion systems (rapid phase separation) would be formed between the DES and *n*-dodecane (or decyl ether). These results implied that the CO₂-responsive emulsion system was more easily formed between the imidazole-based DES and plant oils, which would be useful in the production and conversion of the plant oils.

It is of significant importance to investigate the mechanism on the formation of the CO₂-responsive DES-based emulsion. By carefully analysing the properties of both the prepared DESs and the olive oil, we could deduce that the changes of the DESs' properties after bubbling CO₂ may be the main reason for the observed phenomenon. ATR FT-IR spectra of the DESs before and after the bubbling of CO₂ were conducted to study the adsorbed state of CO₂. As shown in Fig. 3A, the chemically or

physically absorbed CO₂ in the imidazole/EG DES could be clearly distinguished. The new observed peak at 1635 cm⁻¹ after the bubbling of CO₂ could be ascribed to the asymmetric stretching of carbamate, implying the occurrence of chemical absorption of CO₂ by the DES. Meanwhile, a new peak at 2350 cm⁻¹ was found, which was assigned to the asymmetric stretching of the physically absorbed CO₂.^{34,35} More importantly, these two signals disappeared after the removal of CO₂ by the bubbling of N₂, indicating that the DES was completely resumed. Thus, the process to tune the property of DESs with CO₂ was reversible. The same phenomenon was also observed for three other imidazole-based DESs (Fig. S9, ESI[†]).

¹³C NMR spectra were further applied to characterize the imidazole/EG DES before and after the bubbling of CO₂ (Fig. 3B). In comparison with the fresh imidazole/EG, a new peak appeared at 159.2 ppm, which was assigned to -NHCOO-, confirming the chemically bonded CO₂.^{32,36,37} Another new peak was found at 67.2 ppm, further implying the formation of carbamates after the bubbling of CO₂.³⁶ These results confirmed the chemically bonded CO₂. Consistent with the results of ATR FT-IR spectra, the two peaks would vanish after the removal of CO₂. Interestingly, the intensity of the C2 peak decreased due to the bonding of a N(1) atom with CO₂.³⁶ For the other three imidazole-based DESs, similar results were also obtained (Fig. S10, ESI[†]).

Furthermore, the conductivity of the prepared imidazole-based DESs before and after the bubbling of CO₂ was determined (Fig. 3C). The conductivity was significantly increased after the bubbling of CO₂ because of the formation of cations and anions between CO₂ and imidazole in the form of carbamates. The change in the conductivity for the imidazole/EG DES, which increased from 31.2 to 2000 μS cm⁻¹, was particularly obvious. In agreement with the results from ATR FT-IR spectra and ¹³C NMR spectra, the conductivity value was restored after the removal of CO₂ by N₂, further suggesting the reversibility of the process.

On the basis of the above results and some reported knowledge,^{26,28,35,36} a possible mechanism was proposed for the formation of the CO₂-responsive DES-based emulsion (Fig. 3D). First, the emulsion can be generated by stirring a mixture of the fresh imidazole/EG DES and olive oil, and the formed emulsion was stable under ambient conditions. Then, after the bubbling of CO₂ into the formed emulsion, CO₂ would interact with the N atom in the imidazole to form cations and anions (Fig. 3D), which would significantly increase the polarity of the used DESs. Consequently, phase separation would occur because too high polarity was unbeneficial for forming a stable emulsion. Finally, after removing CO₂ by the bubbling of N₂, the properties of the DESs were restored, and thereby, the emulsion would be re-formed after stirring the mixture.

In summary, the concept of CO₂ switchable DESs was proposed and a family of imidazole-based DESs with low viscosity and low melting point were designed. It was found that the properties of these obtained DESs could be easily tuned by CO₂. A CO₂-responsive emulsion could be generated between the developed DESs and olive oil: complete phase separation of

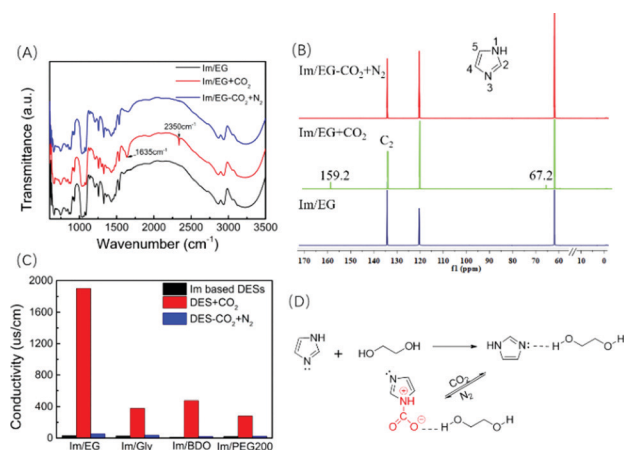


Fig. 3 ATR FT-IR spectra (A) and ¹³C NMR spectra (B) of the imidazole/EG DES, (C) conductivity of the prepared imidazole-based DESs, and (D) a proposed mechanism for the formation of the CO₂-responsive DES-based emulsion.

the emulsion occurred with CO₂, while the emulsion would be resumed after removing CO₂. The mechanism studied revealed that the reversible formation of cations and anions between CO₂ and the imidazole in the form of carbamates afforded the emulsion having a CO₂-responsive property. This CO₂ switchable system has great potential applications in the fields of dissolution and easy separation.

The authors thank the National Natural Science Foundation of China (21773307 and 21873012) for financial support.

Conflicts of interest

There are no conflicts to declare.

Notes and references

- 1 C. J. Clarke, W.-C. Tu, O. Levers, A. Bröhl and J. P. Hallett, *Chem. Rev.*, 2018, **118**, 747–800.
- 2 H. Wang, Y. Zhao, F. Zhang, Y. Wu, R. Li, J. Xiang, Z. Wang, B. Han and Z. Liu, *Angew. Chem., Int. Ed.*, 2020, **59**, 11850–11855.
- 3 A. Farrán, C. Cai, M. Sandoval, Y. Xu, J. Liu, M. J. Hernáiz and R. J. Linhardt, *Chem. Rev.*, 2015, **115**, 6811–6853.
- 4 E. L. Smith, A. P. Abbott and K. S. Ryder, *Chem. Rev.*, 2014, **114**, 11060–11082.
- 5 D. V. Wagle, H. Zhao and G. A. Baker, *Acc. Chem. Res.*, 2014, **47**, 2299–2308.
- 6 P. H. Wadekar, R. V. Khose, D. A. Pethsangave and S. Some, *ChemSusChem*, 2019, **12**, 3326–3335.
- 7 Q. Liu, X. Zhao, D. Yu, H. Yu, Y. Zhang, Z. Xue and T. Mu, *Green Chem.*, 2019, **21**, 5291–5297.
- 8 P. Jaumaux, Q. Liu, D. Zhou, X. Xu, T. Wang, Y. Wang, F. Kang, B. Li and G. Wang, *Angew. Chem., Int. Ed.*, 2020, **59**, 9134–9142.
- 9 R. Sviigelj, N. Dossi, R. Toniolo, R. Miranda-Castro, N. de-los-Santos-Álvarez and M. J. Lobo-Castañón, *Angew. Chem., Int. Ed.*, 2018, **57**, 12850–12854.
- 10 F. Liu, Z. Xue, X. Zhao, H. Mou, J. He and T. Mu, *Chem. Commun.*, 2018, **54**, 6140–6143.
- 11 D. J. Cronin, X. Chen, L. Moghaddam and X. Zhang, *ChemSusChem*, 2020, **13**, 4678–4690.
- 12 W. Wan, D. Xiong, Q. Zhang and J. Wang, *ACS Sustainable Chem. Eng.*, 2019, **7**, 17882–17887.
- 13 A. Imhof and D. J. Pine, *Nature*, 1997, **389**, 948–951.
- 14 C. Plesa, A. M. Sidore, N. B. Lubock, D. Zhang and S. Kosuri, *Science*, 2018, **359**, 343–347.
- 15 R. Röllig, C. Plikat and M. B. Ansorge-Schumacher, *Angew. Chem., Int. Ed.*, 2019, **58**, 12960–12963.
- 16 X. Zhang, Y. Hou, R. Ettelaie, R. Guan, M. Zhang, Y. Zhang and H. Yang, *J. Am. Chem. Soc.*, 2019, **141**, 5220–5230.
- 17 Y. X. Liu, P. G. Jessop, M. Cunningham, C. A. Eckert and C. L. Liotta, *Science*, 2006, **313**, 958–960.
- 18 J. Y. Kim and S. R. Dungan, *J. Phys. Chem. B*, 2008, **112**, 5381–5392.
- 19 S. Marfisi, M. P. Rodríguez, G. Alvarez, M. T. Celis, A. Forgiarini, J. Lachaise and J.-L. Salager, *Langmuir*, 2005, **21**, 6712–6716.
- 20 J. Ma, X. Li, X. Zhang, H. Sui, L. He and S. Wang, *Chem. Eng. J.*, 2020, **385**, 123826.
- 21 P. G. Jessop, D. J. Heldebrant, X. Li, C. A. Eckert and C. L. Liotta, *Nature*, 2005, **436**, 1102.
- 22 D. Xiong, G. Cui, J. Wang, H. Wang, Z. Li, K. Yao and S. Zhang, *Angew. Chem., Int. Ed.*, 2015, **54**, 7265–7269.
- 23 S. L. Desset and D. J. Cole-Hamilton, *Angew. Chem., Int. Ed.*, 2009, **48**, 1472–1474.
- 24 X. Hao, Z. Leng, H. Wang, F. Peng and Q. Yan, *Green Chem.*, 2020, **22**, 3784–3790.
- 25 X. Pei, D. Xiong, Y. Pei, H. Wang and J. Wang, *Green Chem.*, 2018, **20**, 4236–4244.
- 26 G. Cui, M. Lv and D. Yang, *Chem. Commun.*, 2019, **55**, 1426–1429.
- 27 Y. Gu, Y. Hou, S. Ren, Y. Sun and W. Wu, *ACS Omega*, 2020, **5**, 6809–6816.
- 28 K. Zhang, S. Ren, X. Yang, Y. Hou, W. Wu and Y. Bao, *Chem. Eng. J.*, 2017, **327**, 128–134.
- 29 J. F. Fernández-Bertrán, M. P. Hernández, E. Reguera, H. Yee-Madeira, J. Rodríguez, A. Panequea and J. C. Llopiz, *J. Phys. Chem. Solids*, 2006, **67**, 1612–1617.
- 30 L. Hu, L. Chen, Y. Fang, A. Wang, C. Chen and Z. Yan, *Microporous Mesoporous Mater.*, 2018, **268**, 207–215.
- 31 R. K. Ibrahim, M. Hayyan, M. A. AlSaadi, S. Ibrahim, A. Hayyan and M. A. Hashim, *J. Mol. Liq.*, 2019, **276**, 794–800.
- 32 K. R. Harris, L. A. Woolf and M. Kanakubo, *J. Chem. Eng. Data*, 2005, **50**, 1777–1782.
- 33 G. Balakrishnan, T. Nicolai, L. Benyahia and D. Durand, *Langmuir*, 2012, **28**, 5921–5926.
- 34 C. Wang, H. Luo, D. E. Jiang, H. Li and S. Dai, *Angew. Chem., Int. Ed.*, 2010, **49**, 5978–5981.
- 35 C. Wang, H. Luo, X. Luo, H. Li and S. Dai, *Green Chem.*, 2010, **12**, 2019–2023.
- 36 L. Cao, J. Huang, X. Zhang, S. Zhang, J. Gao and S. Zeng, *Phys. Chem. Chem. Phys.*, 2015, **17**, 27306–27316.
- 37 S. Sarmad, J.-P. Mikkola and X. Ji, *ChemSusChem*, 2017, **10**, 324–352.